Effects of Antioxidants on Photodegradation of Wood Flour/Polypropylene Composites during Artificial Weathering

Yao Peng, Ru Liu, and Jinzhen Cao*

The influence of antioxidants and of their compound systems were evaluated relative to the photodegradation of wood flour/polypropylene (WF/PP) composites using ultraviolet accelerated weathering. Six groups of samples were exposed in an accelerated weathering tester for a total duration of 960 h. The surface color, gloss, and flexural properties of the samples during weathering were tested. In addition, the weathered surfaces were characterized by scanning electron microscopy (SEM), differential scanning calorimetry (DSC), and thermogravimetric analysis (TG). The results revealed the following: (1) after weathering, all samples showed significant color fading and gloss change; (2) composites containing antioxidants showed less loss of flexural strength, fewer surface cracks, and better thermal stability after weathering than the control composite; (3) the crystallinity of polypropylene increased in weathered samples due to recrystallization of lower molecular weight polypropylene; and (4) antioxidant 168 (AO-168) was beneficial to color stability at the early stage of weathering, while composites containing 0.2% antioxidant 1010 (AO-1010) and 1.0% AO-168 (AO-1) maintained the highest retention ratios of flexural properties during weathering.

Keywords: Wood flour/polypropylene composites; Antioxidants; Thermal properties; Photodegradation

Contact information: MOE Key Laboratory of Wooden Material Science and Application, Beijing Forestry University, Qinghua Eastroad 35, Haidian 10083, Beijing, China;
** Corresponding author: caoj@bjfu.edu.cn*

INTRODUCTION

Wood-plastic composites (WPCs) have shown significant market expansion in recent years as a replacement for solid wood. They have the advantages of good dimensional stability and durability against fungi and insects during their service life when compared with wood (Kamdem *et al*. 2004; Chaochanchaikul *et al*. 2011), as well as low maintenance requirements. However, weathering is still an inevitable disadvantage of these materials (Stark *et al*. 2004; Bouza *et al*. 2011; Butylina *et al*. 2012a; Teaca *et al*. 2013), especially in outdoor applications.

Weathering can cause chemical and physical changes in the components in WPCs under natural conditions, such as sunlight, moisture, temperature, and biodeterioration from microorganisms. Consequently, WPCs would mostly show color fading, swelling, and deterioration in mechanical properties after weathering (Beg and Pickering 2008; Fabiyi *et al*. 2008). Wood consists of cellulose, hemicelluloses, and lignin. According to previous studies, lignin is more vulnerable to photodegradation and can be degraded into

water-soluble products (Williams 2005). Muasher *et al*. (2006) suggested that the photodegradation of lignin was responsible for photo-bleaching after 250 h of weathering. The photodegradation of polyolefins involves a series of radical-based photochemical reactions via chain scission (Matuana *et al*. 2011), which accelerate the recrystallization process of the polyolefins. The crystallinity of polylefins has an important effect on the physical, mechanical, and thermal properties of WPCs (Lionetto *et al*. 2012). Thus, the determination of crystallinity may be a useful approach for understanding the effect of weathering on properties of WPCs. Some researchers have found that the flexural strength and modulus of WPCs decreased significantly after weathering. Lee *et al*. (2012) studied six kinds of polyolefin-based WPCs and found that all of their crystallinities increased after 100 h of weathering.

Combinations of hindered phenols and phosphorous antioxidants have been widely used as stabilisers, which are reported to have a synergistic effect on improving the durability, as well as physical and mechanical properties in polyolefins (Butylina *et al*. 2012b). Hindered phenols terminate oxidation by trapping alkylperoxy, alkoxy, and alkyl radicals (Scott 1972). Phosphorous antioxidants inhibit degradation reactions by reacting with hydroperoxide groups, carbon-centred, peroxy, and oxy radicals (Pénzes *et al*. 2010). However, the efficiency of phosphorous antioxidants is affected strongly by their chemical composition and thermal stability (Kriston *et al*. 2010). Ojeda *et al*. (2011) reported that sterically hindered phenol and phosphite antioxidant additives added to polypropylene (PP) slowed its rapid photo-oxidative degradation under natural weathering.

In this study, two kinds of antioxidants, namely antioxidant 1010 (AO-1010) and antioxidant 168 (AO-168), were chosen to make wood flour/polypropylene (WF/PP) composites at different compound proportions; the composites were then exposed in an accelerated weathering tester. The objectives of this study were to compare the effects of different compound systems on mechanical and thermal properties of the composites, and to provide insight into the crystallinity changes in PP before and after ultraviolet (UV) radiation exposure.

EXPERIMENTAL

Materials

The compositions of the tested WF/PP composites are shown in Table 1. The wood flour of poplar (*Populus tomentasa* Carr.) with size 60 to 80 mesh was supplied by the Xingda Wood Flour Company, China. Polypropylene (K8303) with a density of 0.9 g/cm^3 was purchased from Beijing Yanshan Petrochemical Co. Ltd., China. The polypropylene had a melting point of 165 °C and a melting mass-flow rate of 1.5 g/10 min at 230 °C.

Two kinds of antioxidants were chosen for use in this study: antioxidant 1010 (AO-1010, $C_{73}H_{108}O_{12}$) and antioxidant 168 (AO-168, $C_{42}H_{63}O_3P$), supplied by BASF Ltd., Germany. The chemical structures of the two antioxidants are shown in Fig. 1, and their total loading level was maintained at 1.2 wt% WF and PP.

Table 1. Compositions and Labelling of the Studied Formulations

Labels	AO-1010 (wt%)*	AO-168 (wt%)*	WF (wt%)	PP (wt%)
C (control)	0	0	40	60
1010	1.2	0	40	60
168	0	1.2	40	60
AO-1	0.2	1.0	40	60
AO-2	0.4	0.8	40	60
AO-3	0.6	0.6	40	60
*The loading levels of the antioxidants were based on the total weight of WF and PP				

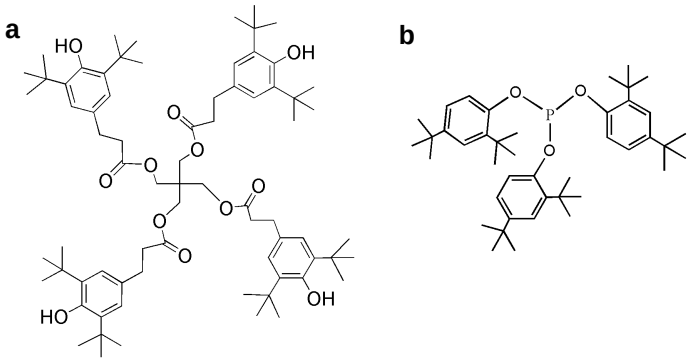

Fig. 1. Chemical structures of (a) AO-1010 and (b) AO-168

Methods

Processing

Prior to manufacturing, the WF was dried in an oven at 103 ± 2 °C until the weight was constant. The PP, WF, and the combined antioxidants were then weighed and mixed in a high-speed blender before being melt-blended in a co-rotating twin-screw extruder (KESUN KS-20, Kunshan; China). After extrusion, the extrudates were cut into small particles of approximately 1 mm and then dried again before the hot pressing process. A hot press (SYSMEN-II, manufactured by the Chinese Academy of Forestry) was used to compress the mat at 180 °C with a pressure of 4 MPa for 6 min. After that, the formed mat was pressed at 4 MPa for another 6 min at room temperature in a cold press. The dimensions of the WF/PP composites were 270 mm × 270 mm × 3 mm, with a target density of 1.0 g/cm^3.

Accelerated UV weathering test

The resistance of the WPC specimens to photodegradation was tested in a QUV accelerated weathering tester (QUV/Spray, Q-Lab Co.; USA) equipped with Q-Lab fluorescent UVA-340 lamps. Tests were carried out according to ASTM G154 (2004) and for up to 960 h (80 cycles). Each cycle consisted of 8 h of UV radiation exposure at 60 °C followed by water condensation at 50 °C for 4 h. The UV-radiation intensity was 0.89 W/m^2 at a wavelength of 340 nm.

Color measurements

The surface color of the WPC specimens before and after weathering was measured with a chroma meter (Datacolour DF 110, Germany). The CIE L*a*b* color system was used to measure the surface color in L^*, a^*, b^* coordinates based on a D65 light source with the observation system of d/8. These three coordinates were used to calculate the total color change, ΔE, using the following equation,

$$\Delta E = (\Delta L^{*2} + \Delta a^{*2} + \Delta b^{*2})^{1/2} \quad (1)$$

where ΔL^*, Δa^*, and Δb^* are the differences between the initial and final values of L^*, a^*, and b^*, respectively. The surface color for three independent specimens was measured at four different positions on each specimen. The measurement area was 40 mm square at the center of each sample.

Scanning electron microscopy (SEM)

Scanning electron micrographs of WPC samples were obtained on a scanning electron microscope (Hitachi S-3400, Japan) operating at an accelerating voltage of 5 kV. Sections of the samples were cut into pieces approximately 5 mm × 5 mm, and the weathered surfaces were sputter-coated with an ion-sputtering device and analyzed at a magnification of 100x.

Surface gloss measurements

Surface gloss of the composites during weathering was measured with a glossmeter (KGZ-1B, Tianjin, China) according to the ASTM standard D2457 (2003), with a test angle of 60°. The measured results were expressed in gloss units (GU). Gloss values for each sample were averaged from measurements on four different locations, one of which was at the center of the samples.

Flexural and impact properties

The modulus of elasticity (MOE) and modulus of rupture (MOR) of unweathered and weathered samples were determined according to Chinese standard GB/T 17659 (1999). The MOR and MOE data were obtained by the three-point static bending test with a loading speed of 5 mm/min (in thickness dimension). Prior to the tests, samples of size 60 mm × 25 mm × 3 mm were conditioned at 26 ± 1 °C and 65% relative humidity for 48 h. The weathered surface of the samples was placed downward. Four samples of each group were tested and the average values were reported. The retention ratios of MOR and MOE of the WPCs after accelerated UV weathering were defined as follows,

$$MOR_{ret.\ ratio} = 100\ (MOR_t/MOR_0) \quad (2)$$

$$MOE_{ret.\ ratio} = 100\ (MOE_t/MOE_0) \quad (3)$$

where MOR_t and MOE_t are the moduli after weathering time t and MOR_0 and MOE_0 are the moduli before exposure.

Differential scanning calorimetry (DSC)

The thermal behavior of samples before and after weathering was determined using DSC (DSC-204; Netzsch, Selb, Germany) equipment. Before analysis, the irradiated surfaces (~50 μm thick) were removed from the weathered specimens by a sharp razor blade. The powders were encapsulated in aluminum pans and heated from room temperature to 250 °C at a heating rate of 10 °C/min under a constant argon flow (60 mL/min). The values for melting temperatures (T_m) and fusion enthalpies (ΔH_m) were determined. The degree of crystallinity (X_c) was estimated by the following equation (Mathew *et al*. 2006):

$$X_c\,(\%) = (100 \times \Delta H_m)/\,(\Delta H_m^0 \times w\,) \quad (4)$$

where X_c is crystallinity (%), ΔH_m^0 is the enthalpy of melting 100% crystallized PP (which is equal to 148 J/g), ΔH_m is the enthalpy required for melting each sample, and w is the weight fraction of PP in WPC composites.

Thermogravimetric analysis (TGA)

Thermal decomposition behaviors of the composites before and after weathering were evaluated by thermogravimetric analysis (Netzsch STA-409, Germany). Samples with a mass of approximately 6 mg were placed in aluminum pans. The temperature range scanned was from room temperature to 600 °C, under constant argon flow.

RESULTS AND DISCUSSION

Color Analysis during Weathering

Quantified color changes in lightness (ΔL^*) and total color change (ΔE) of WF/PP composites containing different compound systems during weathering are listed in Table 2. Throughout the development of the weathering process, it can be clearly seen that the values of ΔL^* in all groups increased.

Table 2. Color Parameters for All Groups of WF/PP Composites during Weathering

Labels	ΔL^*				ΔE		
	240 h	480 h	960 h		240 h	480 h	960 h
C	45.65	52.25	56.27		49.66	56.41	61.64
1010	44.60	61.23	65.12		46.60	65.14	68.90
168	41.65	46.32	62.62		43.75	48.06	66.45
AO-1	40.82	49.68	61.75		42.75	50.97	66.32
AO-2	47.63	52.91	64.86		49.41	55.85	68.49
AO-3	47.96	58.68	65.05		50.40	61.29	68.85

The increase in lightness with exposure time can be attributed to the protrusion of WF on the degraded surface. In wood, lignin is more vulnerable to UV light compared to the other main components (Beg and Pickering 2008). It can undergo complex

photochemical reactions and finally be degraded into water-soluble components. These degradation products resulted in a cyclical erosion of the surface as the lignin was degraded and subsequently washed away, exposing more lignin to degradation. Cellulose was more stable than lignin against UV light, and it became the main part on the degraded surface after weathering. Cellulose is white in color; therefore, the values of lightness on the weathered surface increased.

After weathering for 240 h, the values of ΔL^* in 168, 1010, and AO-1 groups were lower compared to the control composite, suggesting that AO-168 alone and AO-1010 at higher loading levels were beneficial to color stability of the composites at the early stage of weathering. The AO-1010 is a type of phenolic antioxidant, which can donate a hydrogen atom to free radicals and produce hydroperoxides and quinoids, slowing down the degradation and discoloration of WF. As for AO-168, it is a type of phosphite antioxidant and can eliminate quinones and change into an achromous aryl phosphate. Therefore, the combination of two such antioxidants worked synergistically and alleviated the photo-bleaching of WPCs effectively during the first 480 h of weathering. However, such effect was weakened with extended exposure time, for both the ΔL^* and ΔE values in composites containing antioxidants were higher than that in the control sample at the end of weathering. This phenomenon can be attributed to the products originating from the photo-reactions of the antioxidants, which contained chromophoric groups, such as carbon-carbon double bonds, carbonyl groups, and paraquinones, which promoted discoloration of WPCs (Fabiyi *et al*. 2009). The changes of ΔL^* in AO-2 and AO-3 groups were similar to the AO-1 group but less pronounced due to their higher content of AO-1010. The reaction products of AO-1010 cannot be decomposed by adequate AO-168 and resulted in more obvious surface discoloration, which can explain the higher values of ΔL^* and ΔE after longer exposure time.

The changes in ΔE values for all composites were found to be consistent with the changes in ΔL^* values. All results indicated that both antioxidants and compound systems protected WPCs from discoloration in the early stages of weathering. Both 168 and AO-1 groups seemed to be the most effective groups in retarding color change during weathering.

Surface Morphology Analysis by SEM

Figure 2 shows SEM images of all composites before and after weathering for 240, 480, and 960 h. All composites showed smooth surfaces before exposure. After 240 h of weathering, some voids and fine cracks appeared in the control group. With the increase of weathering time, the amount of cracks and WF increased on the weathered surfaces. After 480 h exposure, the degradation of the surface layer was more serious in the control, 168, and 1010 groups than the composites containing compound systems, demonstrating a synergistic action of AO-168 and AO-1010.

It seemed that the efficiency of antioxidants vanished after being weathered for 960 h, because the surface morphologies of all composites changed drastically. The number and frequency of the cracks increased, and numerous cracks can be found in the polymer matrix. Moreover, WF protruded on the surface of weathered specimens, which made them easily distinguishable. Wood components can swell and shrink after absorbing and desorbing moisture during weathering cycle (Du *et al*. 2010). The PP layer

was also attacked and became more and more brittle under UV-irradiation. These two factors created stress at the WF/PP interface, causing cracks on the weathered surface. During the condensation process, water droplets accumulated on the weathered surface of the samples. With the increase of water droplets, the cracked PP can easily leach from the surface together with water, leading to the protrusion of WF (Fabiyi *et al*. 2009).

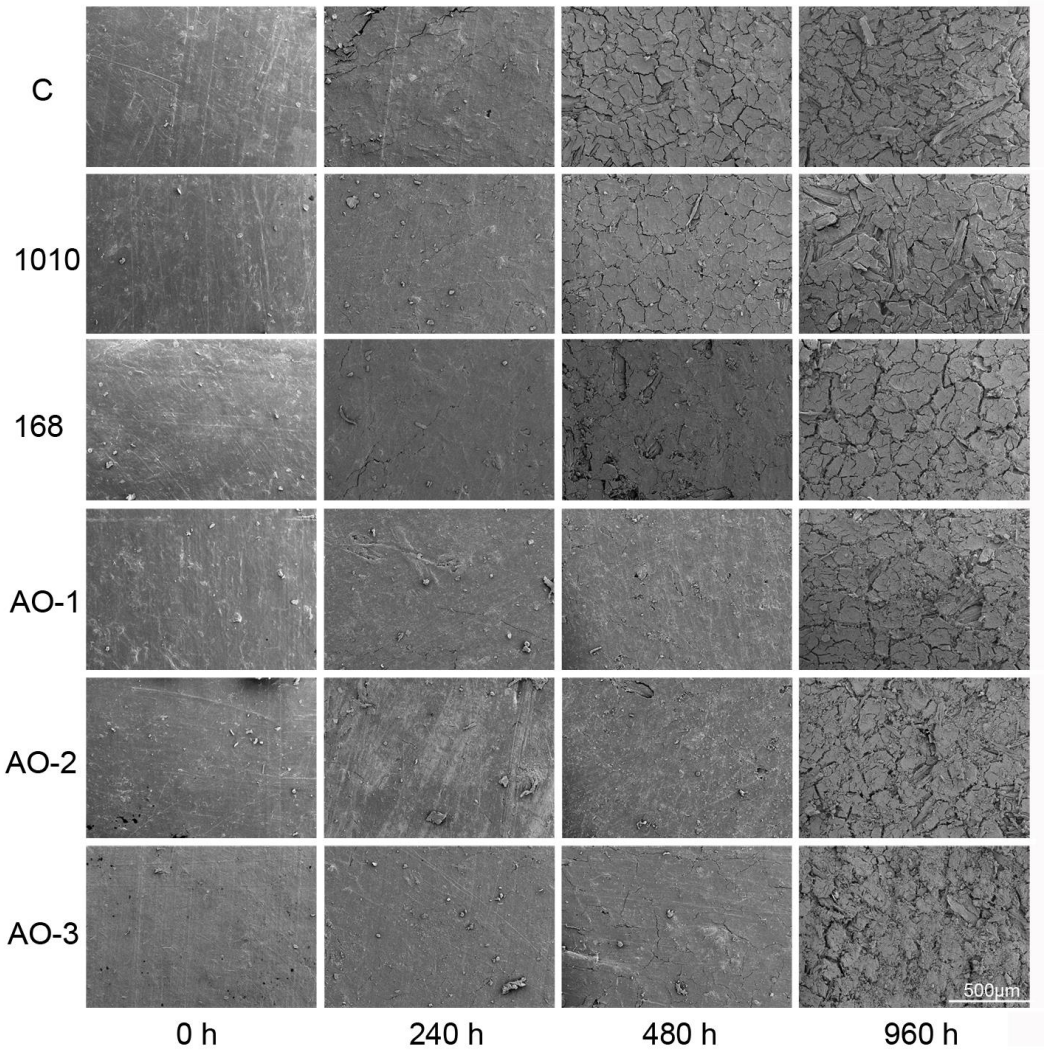

Fig. 2. SEM images of the surface layer of all groups of WF/PP composites

Surface Gloss Analysis

Gloss was determined by the surface reflectivity of a substance, which was also reported to be highly related to the surface smoothness. It can be clearly seen from the SEM results that weathering damaged the samples and made their surface rough. The changes of gloss on the exposed surface during weathering are shown in Fig. 3. Before weathering, the control composite showed higher gloss values, indicating a smoother surface than other samples. The relatively rough surface of the other composites may be due to their poor fluidity during extrusion, resulting from the addition of antioxidants. The gloss decreased during the first 240 h of weathering. After that, values for all groups

decreased significantly with extended weathering time, resulting from the chalking of PP and protrusion of WF on the surface. It should be noted that two groups (labeled as AO-1 and 168) showed higher gloss values between 480 h and 960 h of weathering, which can be attributed to their relatively high amount of AO-168. According to Gugumus (2002), AO-168 readily migrates to the surface due to its low molecular weight, protecting the surface morphology of the weathered samples effectively. The results of surface gloss analysis were consistent with the SEM results (Fig. 2).

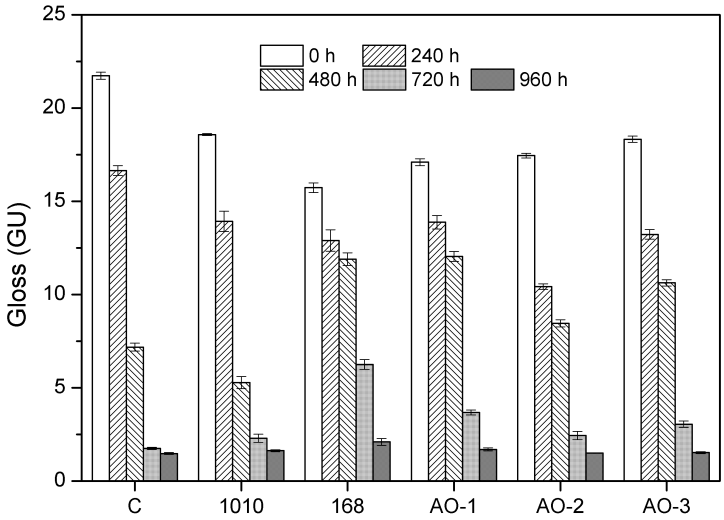

Fig. 3. Change in surface gloss of all groups of WF/PP composites as a function of weathering time. Data expressed as mean ± standard deviation

Mechanical Properties Analysis

Figure 4 illustrates the effects of antioxidants on flexural MOR and MOE for WF/PP composites during UV weathering. Except for the AO-1 group, both the values of MOR (Fig. 4a) and MOE retention ratios (Fig. 4b) decreased after 240 h of weathering, and then increased slightly until 480 h. The parameters seem to change cyclically over a period of 480 h.

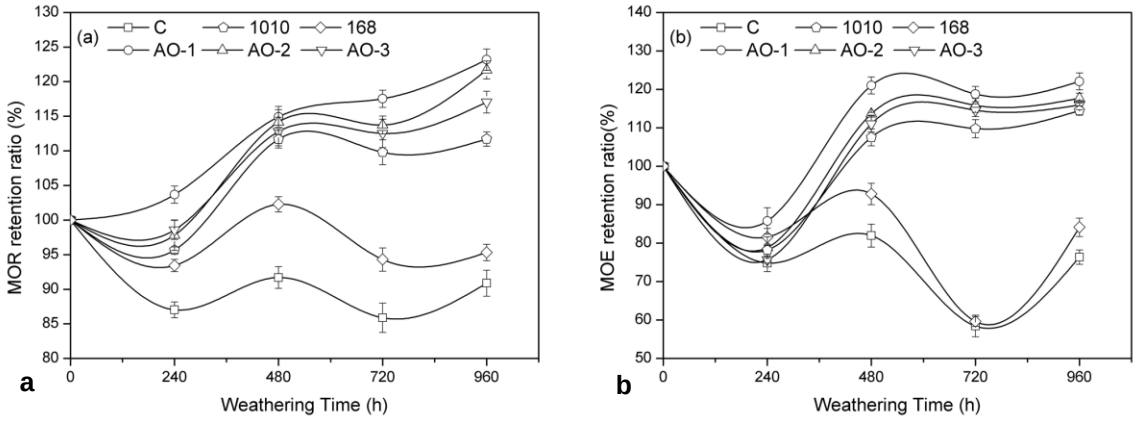

Fig. 4. Change in the (a) MOR retention ratio and (b) MOE retention ratio of all groups of WF/PP composites as a function of weathering time

Four different mechanisms were considered to be responsible for these changes in correspondence to different weathering periods.

The first mechanism was PP degradation. During weathering, PP will degrade through chain scission and form short PP chains. This mechanism will result in the decrease of MOR values and may be the main reason for the decreasing strength from 0 to 240 h. The second mechanism is PP recrystallization. Short PP chains accumulate and form crystalline regions, which should benefit the flexural strength. This is based on the first mechanism, and is closely related to the state of WF on the composite surface. Protrusion of WF on the surface would inhibit the recrystallization of PP. This mechanism may explain the increase of flexural strength during from 240 h to 480 h.

The third mechanism is surface cracks. Severe surface cracks (Fig. 2) resulted in poor interfacial interaction, which might be the main mechanism for the decrease from 480 h to 720 h. The fourth mechanism is WF degradation and leaching. During the condensation of the weathering process, degraded WF accumulating on the surface may leach out, which will benefit the recrystallization of PP. Therefore, the MOR values increased during the period from 720 h to 960 h.

After weathering, the MOR retention ratios of the WPCs were AO-1 (123.2%) > AO-2 (121.7%) > AO-3 (117.0%) > 1010 (111.7%) > 168 (95.3%) > Control (90.9%). Among these, the MOR retention ratio of the AO-1 group increased constantly within the range of this experiment. The MOE retention ratios of all the groups similar to the trend observed for the MOR. Composites containing antioxidants showed better flexural properties than the control group, especially the AO-1 group; therefore, the AO-1 group retained the greatest strength.

Reaction Pathways and Stabilizing Mechanisms of Antioxidants

Based on previous studies and the results above, the anti-oxidant effect of AO-1010 was achieved by donating a hydrogen atom to the free radicals originating from the photodegradation of PP and lignin (Ojeda *et al*. 2011). Therefore, AO-1010 inhibited chain scission of PP, which may explain why the composites containing AO-1010 showed better flexural properties compared to 168 and the control group after weathering (Fig. 4).

As an auxiliary antioxidant, AO-168 can only react with quinones and hydroperoxide, and then change into achromous aryl phosphate. As a result, the composites containing AO-168 exhibited better color stability, especially at higher addition levels.

Polymer Matrix Crystallinity Analysis

The effects of UV weathering on changes in the thermal behaviour of PP were revealed by DSC. The melting temperature (T_m) and crystallinity (X_c) of PP in composites before and after weathering are presented in Table 3.

The differences in crystallinity in composites before weathering were explained by the addition of antioxidants, which may act as a nucleator, accelerating the crystallization process of PP during extrusion.

Table 3. Melting Temperature and Crystallinity of PP in the Samples of WF/PP Composites Before and After Weathering

Labels	Unweathered		Weathered for 960 h	
	T_m (°C)	X_c (%)	T_m (°C)	X_c (%)
C	167.9	19.4	152.4	77.6
1010	166.9	31.8	152.1	96.3
168	168.0	36.1	156.4	66.1
AO-1	167.4	19.2	153.9	75.5
AO-2	167.7	23.8	153.2	85.9
AO-3	168.3	27.8	152.4	86.9

After 960 h of UV exposure, an apparent increase in crystallinity of PP was observed in all groups. The literature reported similar results (Lee *et al*. 2012). This result can well explain the increases in flexural properties due to the recrystallization after 960 h of weathering. Based on a previous study (Beg and Pickering 2008), a large fraction of PP in WPCs was in the non-crystalline state, which allowed the permeability of oxygen into the matrix, resulting in the occurrence of photodegradation. The glass transition temperature of PP is -10 °C, which is below the UV weathering temperature (60 °C) (Windt *et al*. 2011). Therefore, shorter PP molecular chains have better mobility to rearrange into a crystalline phase, which would explain the crystallinity increasing from 19.4% to 77.6% in the control composites after weathering. Since the increase in crystallinity can be used as an indicator for PP chain scission (Zou *et al*. 2008), it can be stated that the crystallinity increments would also reflect the different degrees of surface deterioration.

It should be noted that the 168 group showed the lowest increase in crystallinity of PP compared to other groups after weathering, increasing from 36.1% to 66.1%. This phenomenon can be ascribed to the migration of AO-168 to the surface and its positive effect on retarding the PP chain scission. However, it is interesting that the crystallinity of the PP in the 1010 group increased from 31.8% to 96.3%, indicating that the PP underwent more intensive chain scission during weathering. This may be associated with its products, as well as its chemical structure of ester groups (Fig. 1a), which can improve UV absorption of WPCs. Therefore, with increasing content of AO-1010, the X_c values in compound systems also increased after weathering.

The melting temperature (T_m) of PP in all composites was found to decrease to different extents after 960 h of weathering. The reduction of T_m with exposure time was attributed to a reduction of molecular weight and the breakdown of the PP chains (Joseph *et al*. 2002). The reduction of the T_m for the control composites was approximately 16 °C. However, PP in the 168 and AO-1 groups showed less reduction in T_m than others after weathering.

Thermogravimetric Analysis

The TGA profiles of control composites before and after weathering are presented in Fig. 5a. After 960 h of weathering, the thermal stability of the composite decreased,

which started to decompose earlier than the unweathered composites and left a lesser amount of residue (Fig. 5a). This decrease in thermal stability can be explained by the degradation of both PP and WF as supported by the reduction of the T_m of PP after weathering, as can be observed in Table 3. The residue of the unweathered composites was 19.8%, while it was 8.9% in the weathered composites. This can be attributed to the large amount of lignin in unweathered composites, which acts as a protective barrier and contributes to insulating char formation.

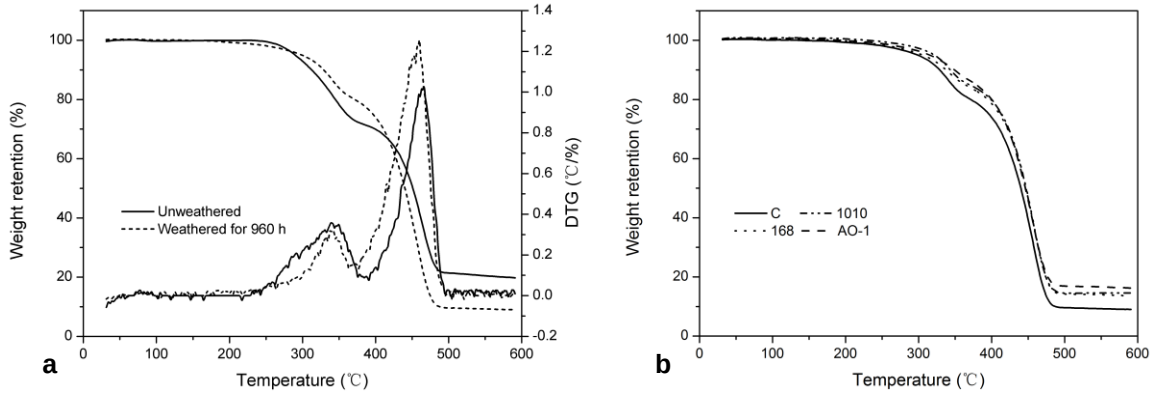

Fig. 5. TGA and DTG curves of (a) control composites and (b) TG curves composites containing antioxidants before and after weathering

The DTG curve of the control composites showed two decomposition steps (Fig. 5a). According to a previous study (Tomczak *et al*. 2007), hemicellulose degrades between 200 and 260 °C, cellulose between 240 and 350 °C, and lignin between 280 and 500 °C. The first decomposition in the range of 220 to 370 °C indicated the decomposition of hemicellulose, amorphous cellulose, and parts of lignin. The second decomposition was observed in the temperature range from 370 to 500 °C. The decomposition of lignin usually can run through the entire temperature range and overlap with the peaks of hemicelluloses and cellulose (Ou *et al*. 2014). The DTG peak of the unweathered sample was observed at 466 °C, while the temperature for the weathered sample was 459 °C. This phenomenon indicates that lignin was degraded and leached from the exposed surface during weathering because lignin is more thermally stable than cellulose and hemicellulose.

The TGA profiles of composites containing antioxidants after 960 h weathering are presented in Fig. 5b. The values of residue were AO-1 (16.2%) > 1010 (14.6%) > 168 (13.6%) > Control (8.9%), suggesting the effectiveness of antioxidants on protecting lignin from photodegradation, especially in the AO-1 group.

CONCLUSIONS

1. Incorporating antioxidants (individually or together) can protect WPCs from UV weathering, although their effectiveness was maintained only over a certain period of weathering. Composites containing antioxidants showed less decrease in surface gloss, flexural properties, and thermal stability than the control group during the

whole weathering. Moreover, fewer cracks were observed on surfaces of the samples containing antioxidants, especially during the first 480 h of weathering.

2. Composites labeled as 168 performed well on color stability, which may be preferred for applications where surface color is of high priority. Compound systems, especially the AO-1 group, had the synergetic effects of the two kinds of antioxidants. Such composites can be used as a load-bearing structure due to the less amount of deterioration on the mechanical properties during the whole exposure process.
3. However, for long-term surface aesthetics of WPCs, pigments might be necessary to further improve their color stability during weathering.

ACKNOWLEDGMENTS

This study was financially supported by the Fundamental Research Funds for the Central Universities (TD2011-14) in China.

REFERENCES CITED

ASTM D2457. (2003). "Standard test method for specular gloss of plastic films and solid plastics," ASTM International, West Conshohocken, PA.

ASTM G154. (2004). "Standard practice for operating fluorescent light apparatus for UV exposure of nonmetallic materials*," ASTM International*, West Conshohocken, PA.

Beg, M. D. H., and Pickering, K. L. (2008). "Accelerated weathering of unbleached and bleached Kraft wood fibre reinforced polypropylene composites," *Polymer Degradation and Stability* 93(10), 1939-1946. DOI: 10.1016/j.polymdegradstab.2008.06.012

Bouza, R., Abad, M. J., Barral, L., Lasagabaster, A., and Pardo, S. G. (2011). "Efficacy of hindered amines in wood flour-polypropylene composites compatibilized with vinyltrimethoxysilane after accelerated weathering and moisture absorption," *Journal of Applied Polymer Science* 120(4), 2017-2026. DOI: 10.1002/app.33306

Butylina, S., Hyvärinen, M., and Kärki, T. (2012a). "Weathering of wood-polypropylene composites containing pigments," *European Journal of Wood and Wood Products* 70(5), 719-726. DOI: 10.1007/s00107-012-0606-y

Butylina, S., Hyvärinen, M., and Kärki, T. (2012b). "A study of surface changes of wood-polypropylene composites as the result of exterior weathering," *Polymer Degradation and Stability* 97(3), 337-345. DOI: 10.1016/j.polymdegradstab.2011.12.014

Chaochanchaikul, K., Jayaraman, K., Rosarpitak, V., and Sombatsompop, N. (2011). "Influence of lignin content on photodegradation in wood/HDPE composites under UV weathering," *BioResources* 7(1), 38-55.

GB/T 17657. (1999). "Test methods of evaluating the properties of wood-based panels and surface decorated wood-based panels," Chinese National Standardization Management Committee, China.

Du, H., Wang, W., Wang, Q., Zhang, Z., Sui, S., and Zhang, Y. (2010). "Effects of pigments on the UV degradation of wood-flour/HDPE composites," *Journal of Applied Polymer Science* 118(2), 1068-1076. DOI: 10.1002/app.32430

Fabiyi, J. S., McDonald, A. G., Wolcott, M. P., and Griffiths, P. R. (2008). "Wood plastic composites weathering: Visual appearance and chemical changes," *Polymer Degradation and Stability* 93(8), 1405-1414. DOI: 10.1016/j.polymdegradstab.2008.05.024

Fabiyi, J. S., McDonald, A. G., and McIlroy, D. (2009). "Wood modification effects on weathering of HDPE-based wood plastic composites," *Journal of Polymers and the Environment* 17(1), 34-48. DOI: 10.1007/s10924-009-0118-y

Gugumus, F. (2002). "Possibilities and limits of synergism with light stabilizers in polyolefins 1. HALS in polyolefins," *Polymer Degradation and Stability* 75(2), 295-308. DOI: 10.1016/S0141-3910(01)00233-6

Joseph, P. V., Rabello, M. S., Mattoso, L. H. C., Joseph, K., and Thomas, S. (2002). "Environmental effects on the degradation behaviour of sisal fibre reinforced polypropylene composites," *Composites Science and Technology* 62(10), 1357-1372. DOI: 10.1016/S0266-3538(02)00080-5

Kamdem, P. D., Jiang, H., Cui, W., Freed, J., and Matuana, L. M. (2004). "Properties of wood plastic composites made of recycled HDPE and wood flour from CCA-treated wood removed from service," *Composites Part A: Applied Science and Manufacturing* 35(3), 347-355. DOI: 10.1016/j.compositesa.2003.09.013

Kriston, I., Pénzes, G., Szijjártó, G., Szabó, P., Staniek, P., Földes, E., and Pukánszky, B. (2010). "Study of the high temperature reactions of a hindered aryl phosphite (Hostanox PAR 24) used as a processing stabiliser in polyolefins," *Polymer Degradation and Stability* 95(9), 1883-1893. DOI: 10.1016/j.polymdegradstab.2010.04.017

Lee, C. H., Hung, K. C., Chen, Y. L., and Wu, J. H. (2012). "Effects of polymeric matrix on accelerated UV weathering properties of wood-plastic composites," *Holzforschung* 66(8), 981-987. DOI: 10.1515/hf-2011-0198

Lionetto, F., Del Sole, R., Cannoletta, D., Vasapollo, G., and Maffezzoli, A. (2012). "Monitoring wood degradation during weathering by cellulose crystallinity," *Materials* 5(10), 1910-1922. DOI: 10.3390/ma5101910

Mathew, A. P., Oksman, K., and Sain, M. (2006). "The effect of morphology and chemical characteristics of cellulose reinforcements on the crystallinity of polylactic acid," *Journal of Applied Polymer Science* 101(1), 300-310. DOI: 10.1002/app.23346

Matuana, L. M., Jin, S., and Stark, N. M. (2011). "Ultraviolet weathering of HDPE/wood-flour composites coextruded with a clear HDPE cap layer," *Polymer Degradation and Stability* 96(1), 97-106. DOI: 10.1016/j.polymdegradstab.2010.10.003

Ojeda, T., Freitas, A., Birck, K., Dalmolin, E., Jacques, R., Bento, F., and Camargo, F. (2011). "Degradability of linear polyolefins under natural weathering," *Polymer Degradation and Stability* 96(4), 703-707. DOI: 10.1016/j.polymdegradstab.2010.12.004

Ou, R., Xie, Y., Wang, Q., Sui, S., and Wolcott, M. P. (2014). "Thermal, crystallization, and dynamic rheological behavior of wood particle/HDPE composites: Effect of

removal of wood cell wall composition," *Journal of Applied Polymer Science* 131 (11), Published Online ahead of Print. DOI:10.1002/app.40331

Pénzes, G., Domján, A., Tátraaljai, D., Staniek, P., Földes, E., and Pukánszky, B. (2010). "High temperature reactions of an aryl-alkyl phosphine, an exceptionally efficient melt stabilizer for polyethylene," *Polymer Degradation and Stability* 95(9), 1627-1635. DOI: 10.1016/j.polymdegradstab.2010.05.031

Scott, G. (1972). "Mechanism of polymer stabilization," *Pure and Applied Chemistry* 30(1-2), 267-290. DOI: 10.1351/pac197230010267

Stark, N. M., Matuana, L. M., and Clemons, C. M. (2004). "Effect of processing method on surface and weathering characteristics of wood-flour/HDPE composites," *Journal of Applied Polymer Science* 93(3), 1021-1030. DOI: 10.1002/app.20529

Teaca, C., Rosu, D., Bodirlau, R., and Rosu, L. (2013). "Structural changes in wood under artificial irradiation determined by FTIR spectroscopy and color measurements – A brief review," *BioResources* 8(1), 1478-1507.

Tomczak, F., Sydenstricker, T. H. D., and Satyanarayana, K. G. (2007). "Studies on lignocellulosic fibers of Brazil. Part II: Morphology and properties of Brazilian coconut fibers," *Composites Part A: Applied Science and Manufacturing* 38(7), 1710-1721. DOI: 10.1016/j.compositesa.2007.02.004

Williams, R. S. (2005). "Weathering of wood," in: *Handbook of Wood Chemistry and Wood Composites*, R. M. Rowell (ed.), CRC Press, Boca Raton, FL, pp. 139-185.

Windt, M., Meier, D., and Lehnen, R. (2011). "Quantification of polypropylene (PP) in wood plastic composites (WPCs) by analytical pyrolysis (Py) and differential scanning calorimetry (DSC)," *Holzforschung* 65(2), 199-207. DOI: 10.1515/HF.2011.024

Zou, P., Xiong, H., and Tang, S. (2008). "Natural weathering of rape straw flour (RSF)/HDPE and nano-SiO_2/RSF/HDPE composites," *Carbohydrate Polymers* 73(3), 378-383. DOI: 10.1016/j.carbpol.2007.12.002

Article submitted: June 8, 2014; Peer review completed: July 23, 2014; Revised version received: July 30, 2014; Accepted: July 31, 2014; Published: August 6, 2014.